Facing the Challenges of the International Airways Volcano Watch: The 2004/05 Eruptions of Manam, Papua New Guinea

ANDREW TUPPER,* IMA ITIKARAI,+ MICHAEL RICHARDS,# FRED PRATA,@ SIMON CARN,& AND DANIEL ROSENFELD**

* *Bureau of Meteorology, Casuarina, Northern Territory, and School of Mathematical Sciences, Monash University, Victoria, Australia*
+ *Rabaul Volcanological Observatory, Rabaul, Papua New Guinea*
# *Cooperative Institute for Meteorological Satellite Studies, University of Wisconsin—Madison, Madison, Wisconsin*
@ *Norwegian Institute for Air Research, Kjeller, Norway*
& *Joint Center for Earth Systems Technology, University of Maryland, Baltimore County, Baltimore, Maryland*
** *Institute of Earth Sciences, The Hebrew University of Jerusalem, Jerusalem, Israel*

(Manuscript received 17 March 2006, in final form 30 May 2006)

ABSTRACT

Devastating eruptions occurred at Manam, Papua New Guinea, from October 2004 to January 2005. An unprecedented set of pilot reports were obtained; ground-, air-, and satellite-observed eruption heights differed greatly. Satellite postanalysis and satellite CO_2 slicing techniques give consistent heights. The climactic eruption, on 27 January 2005, reached 21–24 km MSL; four other eruptions reached 16.5–19 km. Tracking of these ice-rich clouds was done by monitoring strong "ice" signatures on 11–12-μm infrared imagery (for two eruptions), by using reflectance-based techniques (during the daytime), and by using SO_2 detection (available only in postanalysis). A remote lightning detection network could not detect the eruption clouds, despite detecting lightning from thunderstorms in the area. The eruptions appeared to enhance the nocturnal cycle of (ash contaminated) deep convection above the island, consistent with previous work on diurnal volcanic cumulonimbus at Mount Pinatubo. The communications and infrastructure challenges of the region strongly affected the performance of the volcanic ash warning system, but can be partially addressed with the development of appropriate strategies. A strategy of gradual advisory cessation at the end of each event generally worked well but failed where numerical modeling and satellite observation were insufficient. An aircraft apparently encountered SO_2 from the cloud over Dili, Timor-Leste; no engine damage was reported, but no close inspection was made at the time. It is suggested that maintenance guidelines be developed to help clarify the risk of volcanic ash damage from encounters with clouds where only SO_2 odor is observed.

1. Introduction

a. Purpose and structure of this paper

In this paper, we discuss the progress made in the International Airways Volcano Watch (IAVW) since previous writings (e.g., Simpson et al. 2002), in the context of the eruptions of the Manam volcano in Papua New Guinea (PNG). We first introduce the IAVW, the environment of PNG, and the Manam eruptions. We then describe our data and methods, and present an overview of our analysis of the eruption clouds, before discussing their implications for the IAVW. Further work on these eruptions will deal with the seismic and other ground-based analyses of the eruptions themselves, and with the remote sensing results, particularly the SO_2 detection.

b. The development of the IAVW

The IAVW, a set of international arrangements for monitoring and providing warnings to aircraft on volcanic ash in the atmosphere (International Civil Aviation Organization 2006), has been under development since the encounters of four commercial aircraft with the eruption clouds from Galunggung, Indonesia, in 1982 (Johnson and Casadevall 1994).

The IAVW revolves around four key elements: *volcano observatories*, which provide warning and observations of eruptions; *meteorological watch offices,* which write the official warning messages for volcanic ash in the atmosphere (SIGMETs—warnings for speci-

Corresponding author address: Andrew Tupper, School of Mathematical Sciences, Monash University, VIC 3800, Australia. E-mail: a.tupper@bom.gov.au

DOI: 10.1175/WAF974.1

fied phenomena en route); *area control centers,* which control the airspace; and *volcanic ash advisory centers* (*VAACs*), which are specialist regional centers giving advice on the detection and likely dispersion of volcanic ash cloud (International Civil Aviation Organization 2006). As the IAVW has developed, there have been many further encounters between volcanic ash and aircraft (Grindle and Burcham 2003; International Civil Aviation Organization 2001; Simpson et al. 2002; Tupper et al. 2004).

c. The IAVW and Papua New Guinea

The mountainous, volcanically active country of PNG has been problematic for volcanic cloud monitoring since the inception of the IAVW. Both domestic and international aviation (Cantor 1998) have been heavily affected in the past by eruptions from some of PNG's 14 active volcanoes; most notably that of Rabaul in 1994 (Blong and McKee 1995; Rose et al. 1995). The Rabaul Volcanological Observatory (RVO) contends with funding, vandalism, communications, maintenance, and land ownership issues while seismically monitoring these volcanoes. The PNG National Weather Service faces similar challenges performing its meteorological functions.

PNG has a very humid climate and cloudy wet season, rendering remote sensing difficult. The usual infrared "reverse absorption" technique for sensing volcanic ash (Prata 1989a,b) is inhibited by high levels of water vapor in the background atmosphere, and by high levels of ice from the water entrained into or already present in the cloud (Rose et al. 1995). All remote sensing techniques are rendered ineffective if the eruption is obscured by opaque, 17–18-km-high cumulonimbus tops. Tupper et al. (2004), surveying volcanic clouds in the western Pacific, found that the major eruption clouds from PNG were the only ones in the region to not show some utility with the reverse-absorption technique. They suggested an emphasis on developing ground-based infrastructure and on further use of sulfur dioxide (SO_2) detection, to help combat these problems.

d. The 2004/05 Manam eruptions

Manam is an active volcano north of the PNG mainland. It typically has frequent strombolian-style eruptions with a relatively low proportion of fine ash. Eruptions are frequent with a longest known repose period of 9 yr between events, and they typically consist of a series of large paroxysms at intervals of 5–7 days (Palfreyman and Cooke 1976). Figure 1 shows the location of Manam, the principal flight routes, and flight information areas. A high-level eruption cloud in the region can transverse a number of different warning and advisory areas, requiring a complex coordination effort.

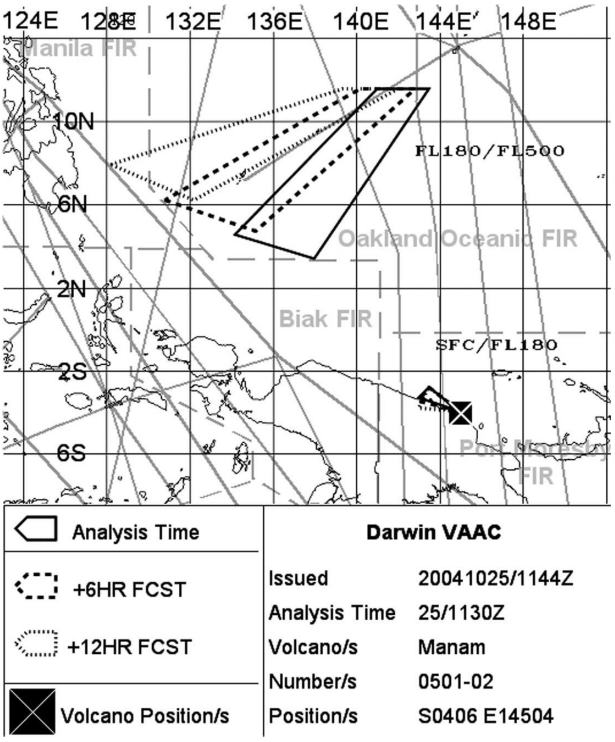

FIG. 1. Example of a "volcanic ash graphic," issued by Darwin VAAC on 25 Oct 2004, overlaid with the principal flight routes (gray solid lines) and the flight information regions (gray dotted lines). The location of the Manam volcano is indicated by the cross, and the black lines indicate the analyzed and forecast positions of the volcanic clouds at altitudes of SFC/FL180 (0–5.4 km MSL) and FL180/FL500 (5.4–15 km MSL).

In October 2004, following a few days of increasing unrest, Manam began erupting, ceasing in the late wet season at the end of January 2005 (a further sub-Plinean eruption in February 2006 is not considered in this paper). Six of the paroxysmal clouds were observed to rise to 10 km or above (Table 1), with the climactic event on 27 January 2005 penetrating well into the stratosphere. Pyroclastic flows reached the coast of the island on several occasions. The effects on the ground were devastating and were most pronounced on the eastern side of the island. Most crops and many villages were wiped out. Only one death on the island was reported; the evacuation of nearly all of the population of ~10 000 to the mainland in late November 2004 apparently prevented further deaths.

The eruptions caused considerable disruption to aviation, with around U.S. $3,000,000 in diversion costs reported to us by one airline alone. Only two aircraft encounters with volcanic cloud have been re-

TABLE 1. Summary of major eruptive events discussed here, maximum heights determined by operational postanalysis and CO_2 slicing techniques, and brief analysis notes for each event.

Event	Postanalyzed height	CO_2 slicing height	Analysis and warning notes
24 Oct 2004: strong strombolian to sub-Plinean eruption; fist-sized scoria damaged villages and pyroclastic flow reached sea	17–18.5 km: minimum observed IR temperature was −69°C, suggesting eruption below tropopause height of 17.5 km; however, the top of the cloud sheared strongly and traveled northward; forward trajectories suggest about 18.5 km	16.5–17 km: could have reached isothermal region near 17.5 km but data inconclusive	Reverse absorption ash signal below freezing level, strong ice and SO_2 signals above freezing level; eruption warning written by RVO on 22 Oct but not sent due to broken fax machine; fast initial SIGMET for low-level eruption but MWO did not receive VAAC advisory of high-level cloud for >6 h; no SIGMETs issued for Biak/Manila FIRs
31 Oct 2004: strong strombolian to sub-Plinean eruption, fine dark-gray to brown ash clouds, scoria to 1-cm size, lava flows	16–16.5 km: highly oblique 0110 UTC *Terra*/MODIS pass shows shadow width >15 km and altitude >14 km; coldest temperature −80°C (near tropopause 16.4 km) suggests 16–16.5 km	16.5–17 km: highest actual value 16.8 km, near model tropopause	No ash signal and ice-rich cloud tops; eruption identified by semicontinuous high-level plume to same altitude as Cb tops; very hard to track plume dispersal because of extensive Cb in area; obvious hot spots with lava flows; SIGMETs issued for Port Morseby FIR
11 Nov 2004: strombolian eruption, ash and scoria fall, lava flows	10–16 km: ground observers reported 8 km MSL; pilots reported column 9 km MSL at 2025 UTC 10 Nov 2004 and 0730 UTC 11 Nov 2004 (Fig. 3j); TOMS SO_2 image shows plume dispersing WSW, matching wind profiles from 10 to 16 km	N/A: plume obscured by cloud	A tropical low to the north (subsequently Typhoon Muifa) extended cirrus canopy over the area, severely inhibiting satellite monitoring; real-time reports from pilots were relayed to RVO, Port Moresby MWO, and Darwin VAAC; no SIGMETs issued as VAAC could not see eruption cloud
23–24 Nov 2004: strong strombolian eruption, lava flows toward but not reaching sea, heavy ash and scoria fall	18–19 km: undercooled overshooting top −96°C on *NOAA-15*/AVHRR at 2040 UTC 23 Nov, surrounding cloud −81°C near center grading to −86°C at edge; undercooled top casts 7-km shadow on umbrella cloud, suggesting ~1 km extra height	16.5–17 km: 0020 UTC 24 Nov image showing extensive cloud near tropopause (approx 16.8 km in model), with no evidence of lasting stratospheric penetration	Activity was identified in real time by 14 h of repeated deep convection developing over Manam; postanalysis shows SO_2 dispersing SE and NE of volcano, consistent with deep tropospheric eruption; SIGMET current for low-level eruption, upgraded 24 Nov after high-level eruption had ceased
19–20 Dec 2004: strong strombolian to sub-Plinean eruption, pyroclastic lava flows not reaching sea	16.5–17 km: deep convection in plume shape, minimum temperature −80°C at 1530 UTC 19 Dec; no obvious stratospheric penetration; pilots reported +30 000 ft (9.1 km)	16.5–17 km: Same arguments as for 31 Oct; highest actual value 16.7 km	Advisories were issued in real time for lower-level eruption, but intensification was only picked up in reanalysis; postanalysis shows SO_2 dispersing west and southwest over Australia and Indonesia; low-level SIGMET issued
27 Jan 2005: sub-Plinean to Plinean eruption at 1400 UTC; widespread debris, with severe damage to observatory at Warisi	21–24 km: overshooting, undercooled eruption column at −71°C, surrounded by warmer −63°C umbrella cloud; edge of cloud at −82°C, tropopause at −85°C; 19°–22°C overshoot into stratosphere	22–23 km: two possible solutions for height, but imagery interpretation highly in favor of stratospheric cloud; no height estimate possible for likely undercooled area	Destruction of ground communications and active monsoon inhibited detection of eruption. First message from Rabaul at 0300UTC 28 Jan; no split-window signal but strong SO_2 dispersing westward over next few days; ashfall reported to west of eruption confirms ash in high-level cloud; one aircraft encounter (Dili, Timor Leste)

ported; while it is tempting to ascribe that to the efficient workings of the IAVW, there have actually been serious difficulties with many of the eruptions.

2. Data and methods

a. Ground and pilot reports

Ground monitoring of the eruptions was generally performed from the village of Warisi on the southeast of the island, using a single seismometer and visual and aural observations. Communications between Manam and RVO are made using high-frequency (HF) radio at prearranged times. High-frequency radio is widely used in PNG and is a cheap and appropriate communications solution; the disadvantage to the system is that it is difficult to make a fast response to unexpected events. In recognition of this and of the timeliness demands that the aviation industry was making, an airline donated a satellite phone and paid ongoing bills during January 2005. Unfortunately, this phone, along with most of the facilities at Warisi, were destroyed during the first opportunity to really test its utility, in the violent eruption of 27 January.

Pilot reports of volcanic eruptions are of variable accuracy, usefulness, and timeliness (Simpson et al. 2002; Tupper and Kinoshita 2003). During the past few years, Air Niugini has developed its own reporting system for pilots (Innes 2004). As a result, an unprecedented number of signed, written pilot reports were collected during the eruptions, all from short-range domestic routes. The written reports were collected at flight dispatch and were kindly provided to the Darwin VAAC for postanalysis. Some pilots also carried cameras to photograph events of interest, and most of the pilots already had at least some familiarity with previous eruptions.

b. Satellite-based height analysis: CO_2 slicing

Cloud-height analysis was carried out in real time using normal operational cloud-top temperature (assuming blackbody radiances) and cloud drift techniques (Holasek et al. 1996; Tupper et al. 2004); major events were then reanalyzed using data not available in real time. These data were then compared with the results of heights derived from CO_2 slicing (Menzel et al. 1983; Wylie et al. 1994). Because this is the first application of CO_2 slicing to volcanic cloud analysis, a brief explanation of the technique is given here. No changes have been made to the algorithm in consideration of volcanic cloud properties for the results presented here.

The CO_2 slicing technique uses five infrared bands available on the Moderate Resolution Imaging Spectroradiometer (MODIS). Four of these bands are located within the 15-μm CO_2 band (bands 33–36; 13.3, 13.6, 13.9, and 14.2 μm, respectively), with the fifth band being the 11-μm window (band 31). The CO_2 slicing method takes advantage of the fact that the CO_2 bands become more transmissive with decreasing wavelength, that is, as the bands move away from the peak of the CO_2 absorption at 15 μm. This behavior is encapsulated by the peaks in the weighting functions (Seemann et al. 2003) for these four CO_2 bands.

The cloud pressure is obtained from the solution of the equation that is derived for a ratio of cloud signals (i.e., the change in radiance caused by the presence of the cloud) for two spectral channels of frequency ν_1 and ν_2 for a given field of view. With $I_m(\nu)$ being the measured cloud radiance and $I_{\text{clr}}(\nu)$ being the corresponding clear air radiance (calculated using a radiative transfer model), this may be written as

$$\frac{I_m(\nu_1) - I_{\text{clr}}(\nu_1)}{I_m(\nu_2) - I_{\text{clr}}(\nu_2)} = \frac{\varepsilon_1 \int_{P_s}^{P_c} \tau(\nu_1, p) \dfrac{dB[\nu_1, T(p)]}{dp}\, dp}{\varepsilon_2 \int_{P_s}^{P_c} \tau(\nu_2, p) \dfrac{dB[\nu_2, T(p)]}{dp}\, dp}, \tag{1}$$

where ε is the cloud emissivity, P_s is the surface pressure, P_c is the cloud pressure, $\tau(\nu, p)$ is the fractional transmittance of radiation of frequency ν emitted from the atmospheric pressure level p arriving at the top of the atmosphere ($p = 0$), and $B[\nu, T(p)]$ is the Planck radiance of frequency ν for temperature $T(p)$. Two fundamental assumptions inherent in this method are 1) the cloud emissivity is the same for both ν_1 and ν_2 and 2) the cloud has infinitesimal thickness.

The cloud signal ratio on the left side of Eq. (1) is determined from radiances measured by MODIS and the National Oceanic and Atmospheric Administration/National Centers for Environmental Prediction (NOAA/NCEP) Global Data Assimilation System (GDAS) gridded meteorological product, with the cloud signal ratio on the right side of Eq. (1) calculated from a forward radiative transfer model (Menzel et al. 1983). The ratios are set up using predetermined combinations of the four MODIS CO_2 bands (Platnick et al. 2003). The cloud pressure that best minimizes the difference between the observed and calculated cloud signals for the four CO_2 bands is considered the most representative. The cloud-top pressure is converted to height from the meteorological profiles in the GDAS product. When no viable solution is obtained from the CO_2 bands, a final estimate for cloud-top temperature is obtained with the 11-μm band radiance, that is, a

black-cloud assumption. For meteorological clouds above 3 km MSL (approximately 700 hPa), cloud-top pressures derived from this method have accuracies to within approximately ±50 hPa (Platnick et al. 2003). Areas of increased uncertainty include optically thin cirrus, multilayered cloud scenes, knowledge of clear-sky surface temperatures, isothermal atmospheres, and temperature inversions. The CO_2 slicing method has considerable difficulty determining cloud-top pressures near the tropopause. This is because of the nature of the cloud pressure function, which remains constant in an isothermal atmosphere (Wielicki and Coakley 1981). Cloud-top heights retrieved by the CO_2 slicing method are therefore limited to altitudes below the GDAS-determined tropopause (which may vary from the true tropopause height). Clouds known to reside above the tropopause are reanalyzed separately.

c. Remote sensing of ash

The application of the reverse-absorption algorithm (Prata 1989a, 1989b) to tropical eruptions in the region is discussed elsewhere (Potts 1993; Tupper et al. 2004). The algorithm is generally successful but cannot identify ash in ice-rich clouds. This method was used in addition to infrared and visible pattern analysis (Sawada 1987) and application of several different enhancements using the 1.6- and 3.9-μm channels (Kinoshita et al. 2002; Schneider and Rose 1994). In the Darwin VAAC, these channels are generally used in their default presentations, that is, with 1.6 μm on a simple black to white scale, and 3.9 μm on a white to black scale and calibrated as an infrared channel, because it is felt that these presentations are relatively straightforward for analysts to use and understand. A series of batch commands on the operational satellite display system [the Man computer Interactive Data Access System (University of Wisconsin—Madison 2005), allows more complex multichannel combinations. Geostationary [*Geostationary Operational Environmental Satellite-9* (*GOES-9*)] and polar-orbiting [NOAA/Advanced Very High Resolution Radiometer (AVHRR)] data were used for real-time ash detection during the eruptions, with additional polar-orbiting Earth Observing System/MODIS data used in the post-analysis.

d. Aerosol contamination in ice-rich cloud

A 3.9-μm reflectance-based particle size algorithm (Rosenfeld and Lensky 1998) was used to study daytime cases of ice-rich volcanic cloud in postanalysis. This algorithm has been widely used for studying the effects of aerosols on moist convection (Fromm et al. 2006; Rudich et al. 2003). Studies of eruption clouds at Mount Pinatubo in 1991 have shown skill in identifying not only the eruption clouds, but also the effect of ash clouds entrained into monsoon convection (Tupper et al. 2005). The algorithm is limited by being daytime only and by using an assumption of spherical particles to derive the particle effective radius r_{eff}, but has the strength of allowing the analyst to study particle size variation with height.

e. Detection of volcanic cumulonimbus

Volcanic cumulonimbus (Cb) are cumulonimbus-type clouds that have their genesis associated with an active volcano (Oswalt et al. 1996; Tupper et al. 2005). The effect of the eruptions on the diurnal cycle of convection at the volcano was analyzed in the same manner as Tupper et al. (2005), by creating 5-km nominal-resolution composites of hourly *GOES-9* infrared brightness temperatures from 24 October 2004 to 30 January 2005. Tupper et al. (2005) excluded tropical cyclone–affected days because of the dominant effect of these systems in the Philippines; this was not necessary for PNG.

f. Sulfur dioxide detection using Total Ozone Mapping Spectrometer and Atmospheric Infrared Sounder

Total Ozone Mapping Spectrometer (TOMS) SO_2 retrievals (Carn et al. 2003; Krueger et al. 1995) were used when available, to help verify warnings, using the assumption that SO_2 and ash were to a large extent collocated (Tupper et al. 2004); although some separation of the two is often observed (e.g., Constantine et al. 2000), we assume that they are not perfectly separated. TOMS aerosol index (Torres et al. 1998) images were also examined, although without success. TOMS has been superceded by the Ozone Monitoring Instrument (OMI); we will consider the OMI results in future work.

The Atmospheric Infrared Sounder (AIRS) is an infrared spectrometer with 2378 channels measuring atmospheric radiance between 3.74 and 15.4 μm. The spatial footprint of an AIRS pixel is roughly 6.7×6.7 km^2 at nadir, increasing to 20.4×11.1 km^2 at the swath edge. The instrument is on board the National Aeronautics and Space Administration (NASA) *Aqua* satellite and is used principally for retrieving vertical profiles of temperature and moisture for weather and climate applications.

Prata and Bernardo (2007) have developed an AIRS

retrieval scheme for obtaining SO_2 column amounts for emissions that reach into the mid- to upper troposphere and above. The scheme makes use of the radiances from the very strong antisymmetric stretch absorption feature of the SO_2 molecule centered near ~7.3 μm (~1370 cm^{-1}) (Prata et al. 2003). This spectral region is much less affected by absorption due to volcanic ash than the 8.6- or the 4-μm regions (these two regions have other advantages, including the ability to probe deeper into the troposphere). The retrieval scheme exploits the high spectral resolution of AIRS by searching for a match between a "library" 7.3-μm spectral shape and a measured shape. The measured shape is determined from AIRS by calculating an absorbance spectrum using a reference pixel; that is, a pixel that is unaffected by SO_2. An integration across the absorbance spectrum is directly related to the total column SO_2 amount. In practice the spectrum is contaminated by water vapor features (the effects of other gases in this spectral region are negligible) and the retrieval scheme employs radiative transfer calculations and a least squares minimization approach to obtain a best fit to the measured spectrum. In general, the scheme has been found to be very stable and accurate to about ±3 matm-cm (±3 Dobson units). As with all infrared measurements, clouds confound the measurements, and retrievals in cloudy conditions tend to be noisier, less accurate, and often not possible. In theory, the AIRS retrievals are more accurate when the SO_2 is above ~3 km, b less interference from water vapor and water clouds.

g. Hot-spot detection

Hot-spot imagery was sourced from several places. As a first guess, Darwin VAAC uses stretched 3.7- or 3.9-μm *GOES-9* or NOAA/AVHRR imagery; while relatively unsophisticated, the use of hot spots in the context of their original image allows immediate identification of cloud obscuration or navigation problems. For more sophisticated analysis, the Hawaii Institute of Geophysics and Planetology's MODVOLC algorithm (Wright et al. 2002) was used.

h. Lightning detection

Following the early success of volcanic lightning detection in Alaska (Hoblitt and Murray 1990), and knowing that lightning has been observed in previous Manam eruptions (Palfreyman and Cooke 1976), for each paroxysm lightning data were checked to see if any associated volcanic lightning had been detected by the Global Position and Tracking Systems (GPATS) used by the Australian Bureau of Meteorology. The system is operated by the same organization as that which set up the successful trials in Alaska, and has a range extending beyond PNG. At that range, the observed polarity and type classification of the lightning are suspect, but the central processing system will display results regardless and does not discriminate among different shapes of lightning "pulses," and so it should be able to detect any sufficiently strong signal from volcanic lightning (D. Bland, GPATS Pty. Ltd., 2005, personal communication).

3. Analysis

a. Eruption height chronology

Figure 2 compares the daily maximum heights of the eruption clouds from postanalyzed satellite data with the heights recorded by Air Niugini pilots, and with (when available) heights reported by the ground-based observer, while Table 1 summarizes our analysis of the major eruption clouds, together with some notes about the eruptions and the performance of the IAVW. Operationally reported eruption heights depend on the position of the observer. The satellite-derived heights of the higher eruptions, where confidence is greatest, are generally far greater than pilot-reported heights, because the pilots from their perspective are generally unable to view the top of the eruption clouds, especially where a spreading umbrella cloud near the tropopause occurs. The ground-based observers, at Warisi only 4 km from the summit, had a severely limited perspective, particularly when ashfall and other visibility factors intervened, and tended to report much lower heights.

The largest divergence in observation came during the monsoonal month of January, when satellite visibility was almost nil and pilot and ground visibility quite limited. The climactic eruption of 27 January occurred at night; ground observers were unable to view the eruption column and were in any case too busy dodging rocks to attempt an observation, and any pilots in the area would have been unsighted.

Figure 2 also shows the volcanic alert level (0–4) assigned by RVO during the period. An aviation color code is available for use in the IAVW (International Civil Aviation Organization 2006). The color code varies between green, yellow, orange, and red for an increasing level of emission or expectation. The aviation industry is interested in the flux of ash into the atmosphere and the altitude that it reaches. The assigned volcanic alert level from RVO, like that of most observatories, is oriented toward the population on the ground and, hence, tended to increase leading up to and during the eruptions.

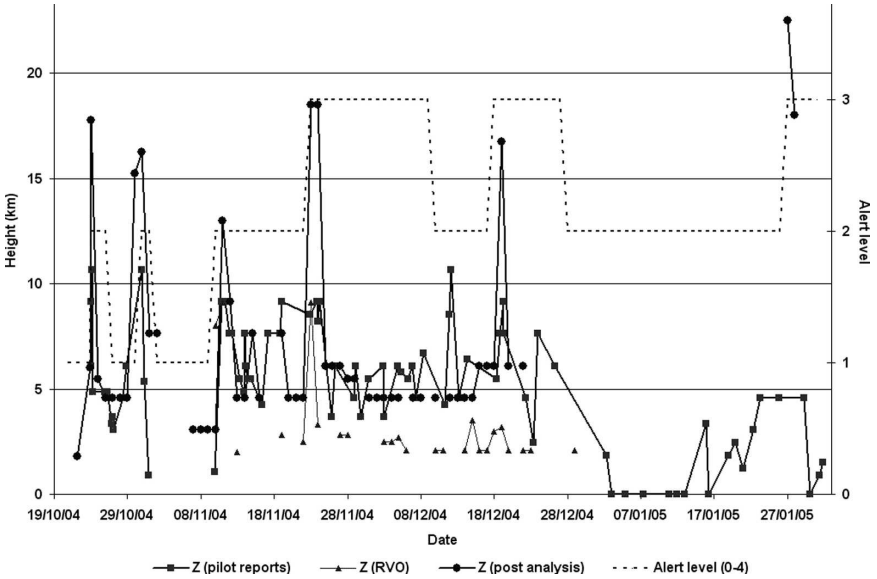

FIG. 2. Summary of daily maximum heights from pilot reports, reported by RVO, and in postanalysis. Where a range of heights is given in Table 1, the midpoint is used. The dashed line indicates the civil alert level recommended in real time by RVO.

b. Analysis of the major eruptions

Table 1 shows a very close correspondence between the heights assigned in postanalysis and the heights derived from CO_2 slicing. Also evident is the strong dynamical role of the tropopause; the cold-point tropopause is usually in the 16–18-km-altitude range during this period.

1) 24 October 2004

Figure 3a captures the first eruption shortly after a high-level cloud developed over the volcano, to a height shown in the CO_2 slicing image (Fig. 3b) of around 17 km. In the reverse-absorption imagery (not shown), the lower-level, obviously ash-rich cloud gave a weak ash signal, while the glaciated, off-white upper-level cloud gave a very strong signature of ice as it expanded. The strength of the positive signal in the reverse-absorption imagery depends on a number of variables, including thermal contrast, smallness of the particles, and viewing angle (Coakley and Bretherton 1982; Prabhakara and Yoo 1990; Rose et al. 1995). Our reflectance-based analysis of the cloud-top particle effective radius (Fig. 3c) does show greatly suppressed particle sizes in the umbrella cloud when compared with a meteorological cloud; this is an indicator of aerosol contamination (Rosenfeld and Lensky 1998).

A few hours later, the eruption cloud was shearing markedly (Fig. 3d). Labels in this figure represent the observed drift of the clouds (arrows), transverse banding that developed as the cloud sheared (1), Kelvin–Helmholtz billows of wavelength ~1 km that apparently formed within the umbrella cloud and are seen through breaks in the top layer of cirrus (2), the main body of ice and SO_2-rich cloud that subsequently moved rapidly northward across the equator (3), and the continuing eruption (4). The CO_2 slicing image here analyses the increasing height of the cloud toward the north (Fig. 3e), consistent with our understanding of the wind fields. A wider view 12 h later (Fig. 3f) shows a chaotic upper cloud pattern dominated by dissipating Cb tops, with new, nonvolcanic convection appearing near the volcano in the bottom left of the image. The AIRS SO_2 contours overlaid in the image show the position of the volcanic cloud; assuming little vertical movement of the cloud in the meantime, the CO_2 slicing technique has successfully picked the height of an eruption cloud that was more than 12 h old.

The 24 October eruption resulted in one aircraft encounter—the minister for intergovernment relations, Sir Peter Barter, had his helicopter windscreen damaged by scoria while overflying the island.

2) 31 OCTOBER 2004

Figure 3g shows a rare, highly oblique view of an eruption column, umbrella cloud, and spreading plume. The eruption column is 3–4 km in diameter. The equivalent CO_2 slicing image (Fig. 3h) suggests that the cloud reached a similar level to previous Cb convection in the area. A shortwave infrared enhancement (Fig. 3i)

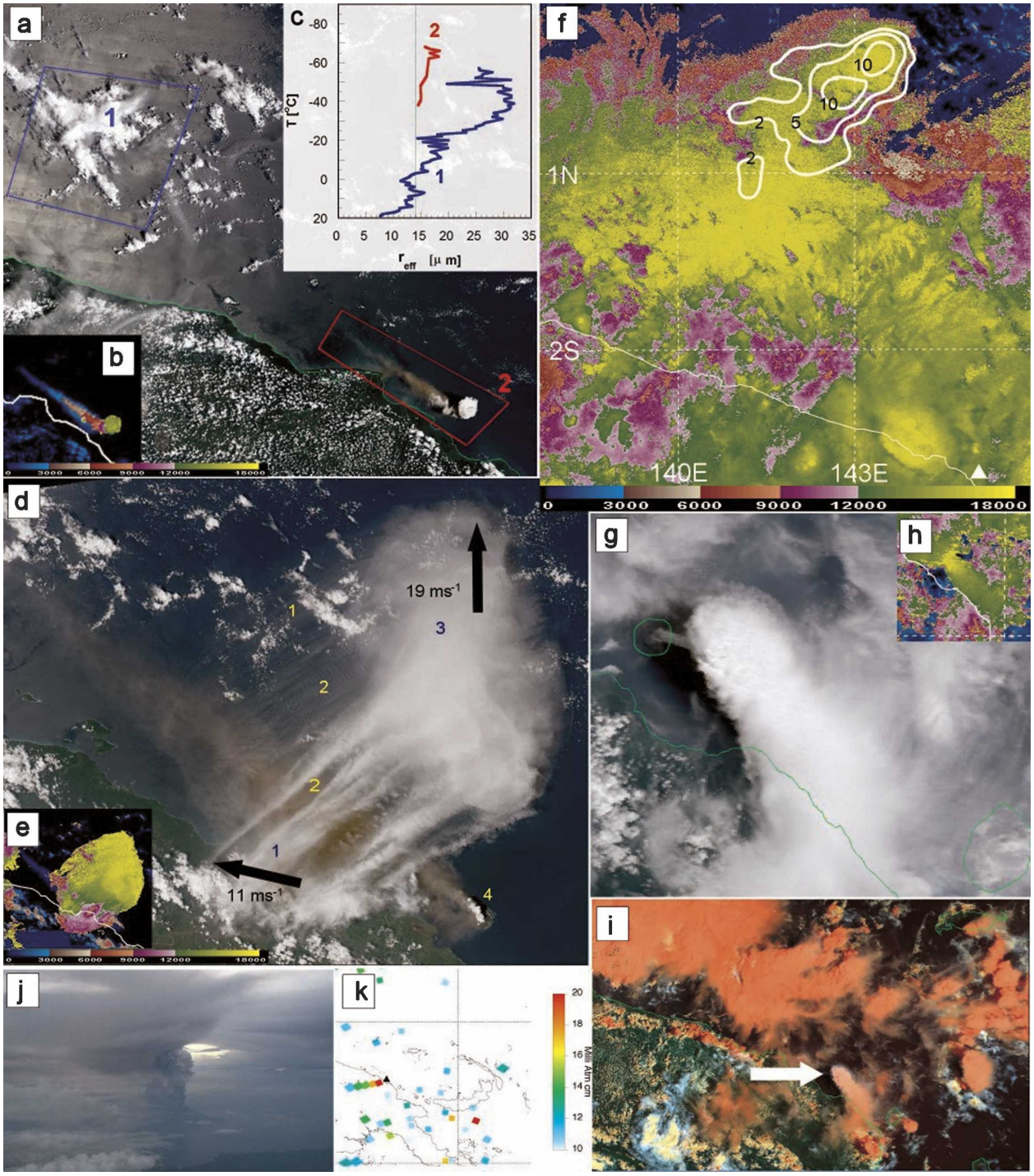

FIG. 3. Manam eruptions in 2004: (a) *Terra*/MODIS true color at 0105 UTC 24 Oct 2004; (b) (inset) derived CO_2 slicing heights for eruption clouds; (c) (inset) cloud-top effective particle radius for areas indicated by 1 and 2; (d) *Aqua*/MODIS true color at 0355 UTC 24 Oct 2004 (see text for description); (e) (inset) matching CO_2 slicing heights; (f) CO_2 slicing heights for 1620 UTC 24 Oct 2004, with derived AIRS SO_2 retrievals contoured in matm-cm overlaid; (g) *Terra*/MODIS true color at ~45° angle to eruption at 0110 UTC 31 Oct 2004; (h) (inset) matching CO_2 slicing heights; (i) matching shortwave infrared composite with 555, 1240, and 2130-nm MODIS channels showing eruption cloud (arrowed) in white; (j) photograph of eruption by Air Niugini pilot (Capt. D. Innes) at 2030 UTC 10 Nov 2004, taken from the south; and (k) TOMS SO_2 retrieval at 0104 UTC 11 Nov 2004.

strongly suggests that aerosols pollute the cloud; the near-white volcanic plume in this enhancement contrasts with the red Cb tops, which have a larger particle size and different near-IR reflectance. Unfortunately, the angle of this image is too oblique to reliably retrieve the effective particle radii (Rosenfeld and Lensky 1998).

3) 10/11 NOVEMBER 2004

The eruption of 10/11 November 2004 was observed from the ground to rise about 8 km MSL (and 9 km MSL by pilots), but satellite observation was almost completely obscured by the cirrus generated from a tropical storm across the equator to the north. Figure 3j shows a pilot's view of the eruption cloud merging into the upper cloud canopy. From the relatively modest plume visible in the TOMS SO_2 imagery (Fig. 3k) and the lack of tops clearly penetrating the cirrus, this appears to have been a smaller event.

4) 23/24 NOVEMBER 2004

A strong strombolian eruption began at 0850 UTC 23 November and ceased at about 2200 UTC. Analysts saw deep convection penetrating the cirrus overcast from 0940 until 2340 UTC; that is, the eruption produced a plume near or above the tropopause for 14 h. Figure 4 shows the top of the eruption cloud in infrared and visible channels; the extensive cloud to the north and northeast is from thunderstorm activity. An overshooting top with "undercooled" pixels in the middle (Holasek et al. 1996) was evident for this and the 27 January 2005 eruptions, but presented little problem for analysts because the undercooled portion is only a few kilometers wide.

Figure 5a shows the dispersion of the large SO_2 clouds produced by the 23 November eruption. Comparison with model winds and CO_2 slicing results (not shown) suggests that the SO_2 dispersions to the SE and SW were at high (11–18 km) and midtropospheric (~10 km) levels, respectively. At the time, the VAACs were focusing on expected movement to the east, where AIRS detected weak levels of SO_2, but TOMS imagery detected substantially more. The relevant ash advisory stated, "Ash is unidentifiable from satellite imagery but is likely to remain in area," and gave a suggested maximum height of 18.2 km [60 000 ft, or flight level (FL) 600 in aviation parlance]. The SW movement of cloud toward Australia was completely unforecast as well as undetected, and reflects a poor observational network and also poor performance by the subsequent numerical model (the Tropical Region Limited Area Prediction System; Davidson and Puri 1992) forecasts and, hence, the dispersion model [the Hybrid Single-Particle Lagrangian Integrated Trajectory model, version 4 (HYSPLIT-4); Draxler and Hess 1998] forecasts as well. Figure 5b shows the perspective of the ground observer and verifies that the eruption column was ash rich.

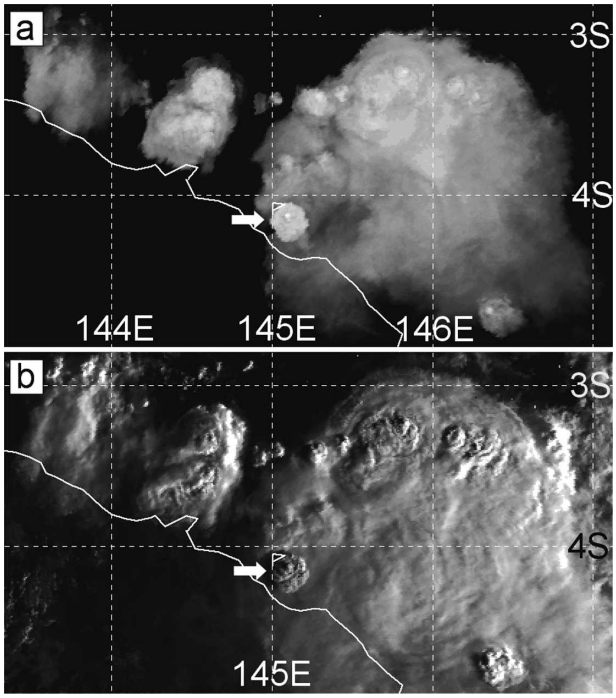

FIG. 4. For the 23/24 Nov 2004 eruption, (a) *NOAA-15*/AVHRR 11-μm contrast stretched image at 2039 UTC 23 Nov 2004 showing the eruption (arrowed) bubbling through cirrus overcast from overnight cumulonimbus convection. The white dot in the center is undercooled overshooting top at −96°C. (b) Matching visible image: the undercooled top casts a 7-km shadow on the umbrella cloud suggesting ~1 km of extra height. Note in both (a) and (b) that other overshooting tops from nonvolcanic convection are apparent.

An aerial photograph (Fig. 5c), taken after the strong eruption had ceased, shows the extent to which the volcano interacted with the moist atmosphere. A dark central eruption column continues, but a tremendous amount of water-rich convection is rising over the hot lava flows to the northeast of the volcano. The cloud wraps around the eruption column and adds water, which then glaciates as the cloud reaches the freezing level (~5 km). The pilot estimated a height of 8.2 km (FL270), which appears reasonable.

5) 19 DECEMBER 2004

Unvalidated OMI imagery (not shown) strongly suggests that cloud from the 19 December 2004 eruption did drift southwestward over West Papua and over

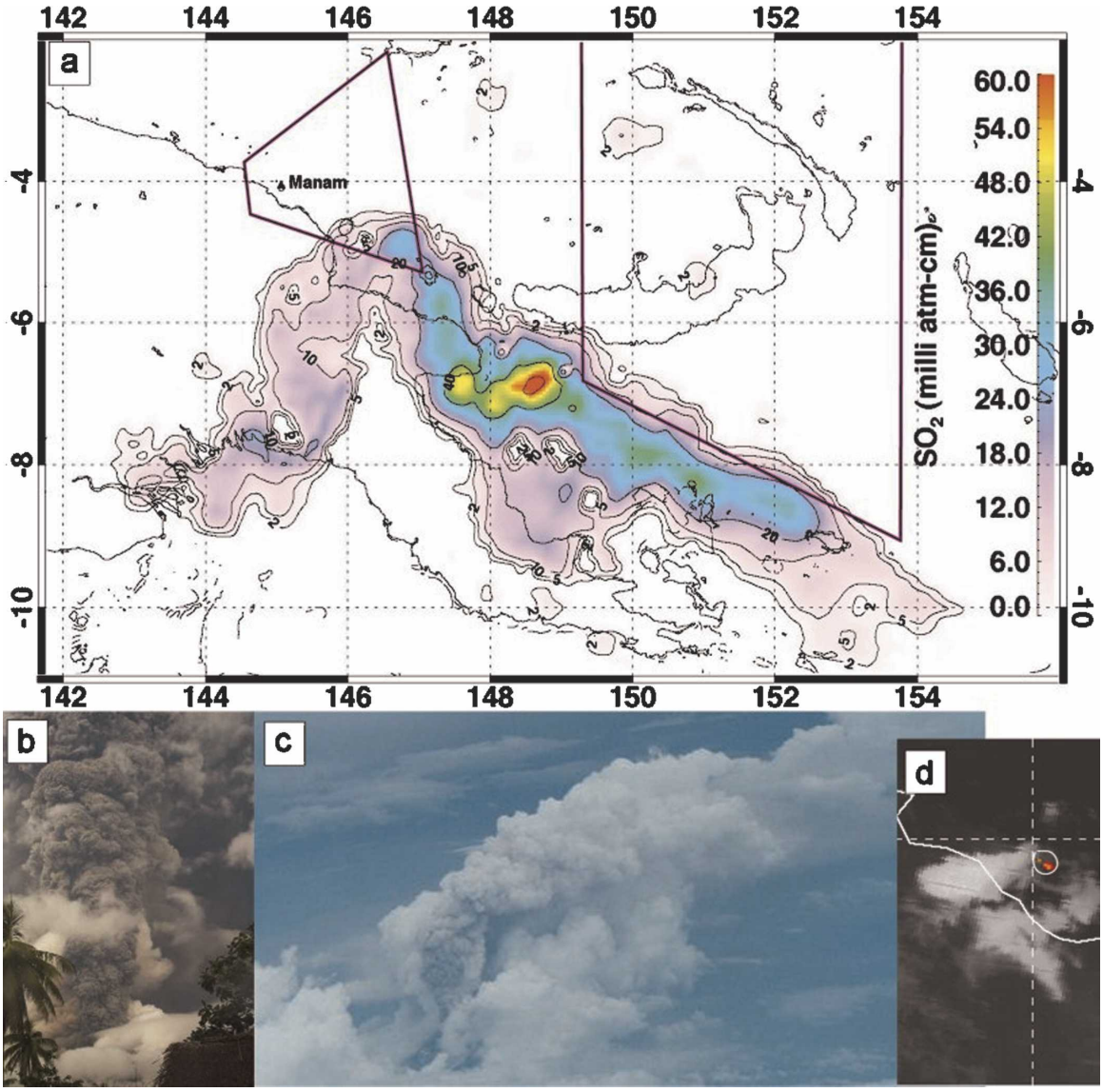

FIG. 5. (a) AIRS SO_2 retrieval at 1535 UTC 24 Nov 2004 overlaid (purple) with 1900 UTC threat areas from Darwin VAAC advisory issued at 1843 UTC; (b) photograph of the eruption from volcanological observer at Manam at 2115 UTC 23 Nov 2004 showing ash-rich eruption column; (c) photograph by Air Niugini Capt. D. Innes taken from the south as the eruption was waning at 0016 UTC 24 Nov 2004; and (d) *Aqua*/MODIS 3.8-μm image at 1530 UTC 19 Dec 2004 showing a plume to the southwest of the eruption and hot spots from lava flow down the southeast valley on Manam.

Australia. Several images of high-level plumes to the southwest were seen by the VAAC, although they were initially missed (on a night shift, when the workload is very heavy) and then postanalyzed the next day. Figure 5d is another oblique MODIS view simultaneously showing the high-level (16.5–17 km) eruption cloud, and the hot spots from lava flows underneath.

6) 27 JANUARY 2005

The climactic eruption at Manam occurred at midnight (1400 UTC) on 27 January 2005; the observation post at Warisi was completely destroyed, and there was no time to try to use the fixed satellite phone or the HF radio communication system as the observer and other villagers were running for their lives; thus, the occurrence and extent of the eruption were not reported until the next day. At the time, the Darwin VAAC was issuing "precautionary advisories" (to warn of the risk of high-level eruptions) every 24 h for Manam, based on RVO's advice. The Darwin VAAC staff were distracted by other duties and did not identify the eruption among the extensive meteorological cloud in real time;

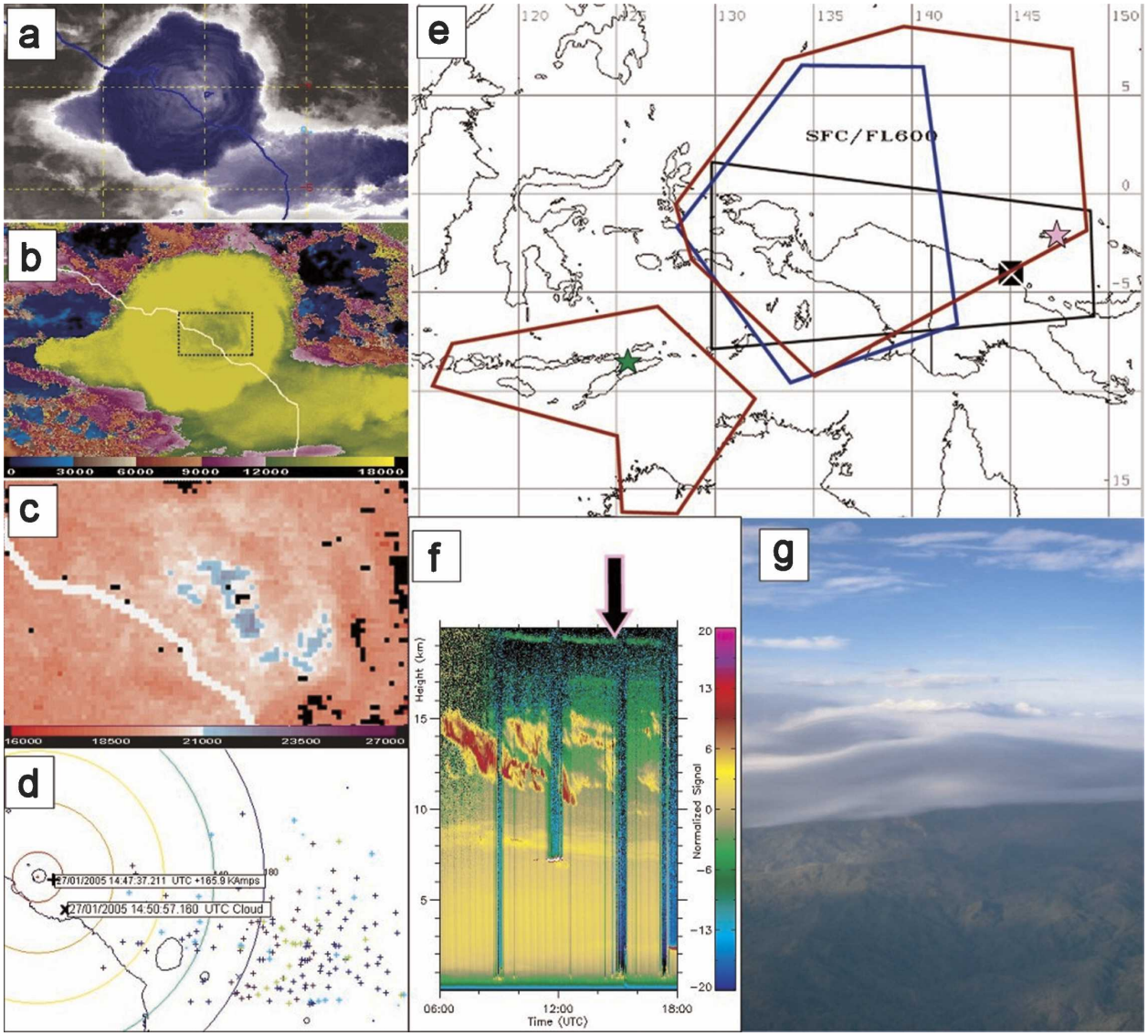

FIG. 6. (a) *Aqua*/MODIS 11-μm image at 1535 UTC 27 Jan 2005; (b) tropospheric CO_2 slicing solution to match (a); (c) stratospheric CO_2 slicing solution for center of the umbrella cloud [boxed area in (b)]; (d) GPATS lightning recordings during the period of the 27 Jan eruption, with two strokes possibly associated with the eruption highlighted; (e) VAAC analysis (black) at 0334 UTC 29 Jan 2005, overlaid by approximate extent of SO_2 AIRS detection at 0441 UTC (blue), and unvalidated OMI detection from 0314 to 0614 UTC (red), where the pink star denotes the ARM site at Manus Island and the green star indicates the location of the aircraft encounter near Dili, 2180 km WSW of Manam, at 2300 UTC 29 Jan 2005; (f) lidar signal from Manus Island showing a layer of aerosols at 19 km MSL (arrowed) on 29 Jan 2005 (courtesy of U.S. ARM program); and (g) photograph of suspected volcanic cloud near Dili (courtesy of P. Lawrie).

the first advisory for the actual eruption was issued at 0347 UTC 28 January 2005, nearly 14 h after the eruption, by which time the leading edge of the cloud had moved well over Indonesia.

The umbrella cloud is shown in Fig. 6a, with an enhancement to highlight the extensive gravity waves and lobate structure (Holasek et al. 1996), and the warm stratospheric intrusion in the center. The extension to the west is part of the eruption cloud, traveling westward at 38 m s^{-1}, and apparently associated with an observed 34 m s^{-1} easterly jet below the tropopause at ~15 km MSL (by contrast, the NOAA global analysis has an easterly jet of 15 m s^{-1}).

The CO_2 slicing analysis suffers from the tropospheric–stratospheric ambiguity in this case, and both solutions are shown for the affected area in the center of the umbrella cloud (Figs. 6b and 6c). At the very center there were a few undercooled pixels where no solution

was possible; otherwise, the estimated heights correspond very well with those estimated using temperature data and a blackbody assumption (Table 1).

Figure 6d shows a lightning detection display, centered on Manam during the eruption. Numerous lightning flashes were recorded to the east in thunderstorm activity; however, only two strokes of lightning (labeled) were recorded near the eruption. Similar results were recorded for all of the major eruptions from Manam in 2004/05. This could be because any volcanic lightning was too weak to be detected by the sensors.

Parts of the cloud could be tracked by the very strong "ice" absorption signature, as in the 24 October 2004 event. However, the cloudscape was chaotic with a great deal of thunderstorm activity, the leading edge of the westerly lobe was very difficult to follow, the operational dispersion model (HYSPLIT-4) had setup problems resulting in an overly small domain, and as a result the VAAC had little confidence forecasting movement farther west of New Guinea. Figure 6e compares the maximum extent of the cloud analyzed by the VAAC with the inferred cloud distribution at that time; although this distribution is based mainly on SO_2 data, a report of ashfall in the Ambunti district 230 km west of Manam implies that ash reached the easterly winds at a level of at least 6 km, and was then transported westward. A layer of aerosols at 19 km MSL was also detected by the micropulse lidar at the U.S. Atmospheric Radiation Measurement (ARM) site on Manus Island on 29 January 2005, coincident with the SO_2 cloud passing overhead (Fig. 6f). This altitude is also consistent with the altitude of the lower parts of the umbrella cloud suggested by Fig. 6c.

An Embraer E120 turboprop aircraft landing in Dili, Timor-Leste, at 2300 UTC 29 January 2005, reported an unusual volcanic aviation encounter:

> On descent into Dili, approaching 10 000 feet (3 km) at 12nm (22 km) aircraft control levers were pulled back to flight idle just prior to entering a thin layer of smooth stratus cloud. Shortly after passing into the cloud, a strange smell was soon noticed in the cockpit. . . the smell became very strong, with high sulphur content. As a precaution the Captain directed the first officer to don his oxygen mask. The smell persisted but began to weaken on descent, and landing was accomplished without incident. After landing, first officer removed the oxygen mask and noted the smell had remained. The captain had by this time become desensitised to the smell. Upon shutdown, unloading was halted, until such time as the cargo hold could be examined for a source of the smell. No smell remained.

Further enquiry revealed that the smell was sharper and more metallic than the odor of H_2S, and was consistent with that of SO_2. The crew had thought the appearance of the cloud unusual enough to take a photograph (Fig. 6g) before entering it and detecting the smell. Nonvolcanic sources of the smell were discussed and dismissed as unlikely. Given that part of the eruption cloud from Manam had just traveled overhead, the most likely explanation is that the observed overnight convection in the area had precipitated ice aggregates containing scavenged SO_2 and possibly other gases (Textor et al. 2003) to the level of the encounter, where the air was above the freezing level, and there the aggregates melted and formed the volcanic fog/stratus noted by the crew. The reported odor desensitization appears to be the first documented case of "olfactory fatigue" (Wunderman 2004) in a volcanic cloud encounter.

c. Volcanic effects on convective cycle

Tupper et al. (2005) describe the effects of the Pinatubo eruption on the convective cycle: convection was enhanced with a clear enhancement and acceleration of the afternoon peak. In practical terms, it is necessary to characterize when ash-bearing thunderstorms are most likely, to structure an aviation avoidance strategy; although no sensible pilot flies through an active thunderstorm in any case, ash left at cruising altitudes by dissipating storms may pose a real risk to aviation.

Figure 7 compares the diurnal cycle of convection over Manam and the nearby island of Karkar during the October–January period of the 2003/04 wet season, when Manam was relatively inactive, against the same period in 2004/05. Both islands have a nocturnal maritime peak in convection that begins about 0300 or 0400 local time (1700–1800 UTC). The processed imagery (not shown) used to derive this graph shows convection moving off the PNG highlands and propagating northward at about 5 m s^{-1} with a peak amplitude offshore to the north, consistent with climatology (Mapes et al. 2003). The comparisons suggest that there may be a modest enhancement of the nocturnal convective cycle, which is the expected result. However, they are not as unambiguous as for Pinatubo; perhaps partially because the nocturnal convective cycle is itself more complex and less understood (Mapes et al. 2003), but also because the Manam eruptions were less extensive than those of Pinatubo, and it is impossible to find a completely eruption-free control year to compare against. Some numerical modeling of the convection may help resolve these issues.

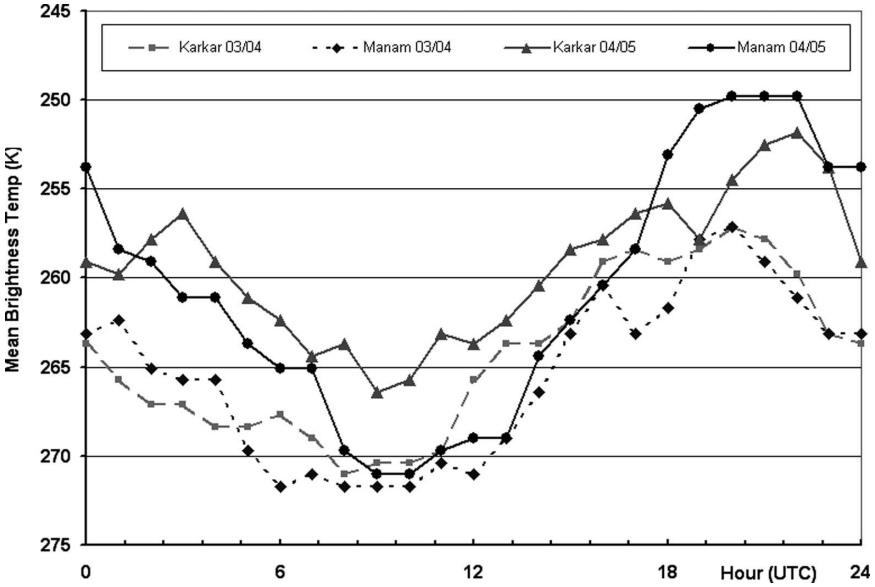

FIG. 7. Mean hourly brightness temperatures from 24 Oct 2003 to 30 Jan 2004 and 24 Oct 2004 to 30 Jan 2005 using *GOES-9* 11-μm data, for Manam and Karkar islands (LT = UTC + 10 h, i.e., 2000 UTC = 0600 LT).

4. Discussion

a. Comparison with the Mount Cleveland, Alaska, February 2001 eruption

Simpson et al. (2002) discussed a number of operational challenges relating to the Mount Cleveland eruption; here, we loosely follow their structure to discuss the progress and remaining issues in these areas.

1) RAPID NOTIFICATION

Notification times from the ground of new eruptions in the sequence depended on HF radio schedules, and did not approach the 5-min time scale often quoted (e.g., Simpson et al. 2002). On the other hand, the ongoing activity and possibility of further large eruptions was clearly signaled by RVO. The precautionary advisories, including an aviation color code warning of red, issued by the VAAC were designed to alert airlines to the possibility of strong eruptions; some airlines in the region took heed and practiced conservative routing, particularly at night. We believe that the surprising lack of serious encounters from the 27 January 2005 eruption can be at least partially attributed to this. Aviation color codes are currently an optional component of volcanic ash advisories and notices to airmen; their mandatory inclusion using the best information available would implement a world-wide standard to be used in precautionary flight planning.

The ad hoc experiment of an airline being provided a satellite phone was a partial success; it enabled easier communications between Manam and Rabaul and it allowed the sponsor airline to save far more money than the cost of the phone by using less conservative routings. Its destruction on 27 January 2005 was unfortunate and leaves some question over its viability as a long-term solution, but the experiment is worth repeating, although preferably with a mobile, rather than fixed, satellite phone. The International Civil Aviation Organization (ICAO) is establishing a more permanent funding arrangement for such communications, where, after appropriate negotiations in the countries concerned, volcano observatories can recover the cost of transmission of warnings to aviation, through the civil aviation authority. It is hoped to apply this arrangement to PNG in the near future. However, there are still likely to be difficulties with the cost of maintaining staff on duty to give instant response to, and notification of, eruptions.

2) SATELLITE-BASED EARLY DETECTION

Satellite-based detection failed for two of the six high-level eruption clouds (19 December 2004 and 27 January 2005) because of nightshift workload issues during a convectively active period, and for one of the eruptions (10 November 2004) because of overlying cirrus cloud. Automated infrared techniques (Watkin et al. 2003) may have detected two of these eruptions, but with a high false alarm rate.

Hot-spot detection of the eruptions themselves was effective for most of the eruptions, providing a similar lead time to the increasing seismicity in the prelude to the 24 October 2004 eruption. However, no hot spots were sensed at all during January 2005, including during the climactic eruption of 27 January, because of the heavy cloud cover.

3) Plume height assignment

There were definite differences in the cloud heights reported from different sources. Tupper and Kinoshita (2003) suggested that "ground-based reports of eruption clouds above 5 km MSL should be taken as being to tropopause height unless there is evidence to the contrary"; the evidence presented here suggests that, in convectively unstable conditions, any moderate to strong eruption can surpass the tropopause height, and a default height assignment based on seismicity should be very conservative even where no ground or pilot observation is made.

Of particular note is the close correspondence in Table 1 between the heights derived from CO_2 slicing and those from operational postanalysis, suggesting that, for as long as CO_2 slicing channels are supported on satellites, the technique can be a very useful technique for measuring the heights of even very thin and old volcanic clouds. All compared heights were within the presumed ± 50 hPa accuracy (Platnick et al. 2003), with only one (24 October 2004) outside a 25-hPa difference.

For many long-running eruptions, it may be possible to improve ground-based height reporting by seconding a meteorological observer in an appropriate location; for example, during the October 2005 Garbuna eruption, the PNG National Weather Service agreed to include volcanic cloud heights in hourly observations from Hoskins Airfield at Cape Hoskins, Gabubu.

4) Reliance on reverse-absorption (split window) technique

The Manam eruptions reinforce the difficulties posed by ice-rich eruptions. On the negative side, ash was certainly present in the eruption columns, but was not explicitly detected *above* the freezing level in any remote sensing—not even by the TOMS aerosol index images that we examined, which had shown success in a previous study (Tupper et al. 2004). Seawater interaction (Mayberry et al. 2003; Rose et al. 1995) could only have been a factor in one or two of the eruptions; consequently, it appears that the relatively low fine-ash content of the clouds, combined with a high water content from the eruptive mixture and from entrained air, is sufficient to completely mask the ash upon freezing. On several occasions, it was almost impossible to forecast the movement of the clouds because of poor model analysis and forecasts.

However, SO_2 imagery was extremely successful in tracking the clouds in postanalysis, infrared pattern recognition served as a good first-guess, and the clouds from the 24 October 2004 and 27 January 2005 eruptions could be tracked by following the highly positive reverse-absorption signature. Reflectance-based shortwave infrared imagery was a very useful technique for diagnosing aerosol contamination of the ice-rich clouds. Operational implementation of SO_2 detection (Carn et al. 2003; Prata et al. 2003), combined with best-practice daytime reflectance-based techniques, continues to offer at least a strong partial solution to the problem.

5) Coordination

Coordination continues to offer many challenges, especially when an ash cloud crosses multiple flight information regions. In the structure of the IAVW, the VAACs inevitably will take on a coordination role, because there are only nine specialist VAACs, as opposed to many Meteorological Watch Offices (MWOs) and Area Control Centres (ACCs). After the 24 October 2004 eruption, when 6 h passed before it was realized that the Port Moresby MWO had not received the VAAC advice of a high-level eruption in response to the low-level SIGMET, a guideline was introduced in the VAAC that, if possible, telephone contact should be made with each affected MWO.

6) Distribution of pilot reports and reporting of encounters

The written pilot record of these eruptions is unprecedented; however, only about 5% of these reports reached Darwin VAAC through the World Meteorological Organization Global Telecommunication System. Many of these reports were recorded at times when the VAAC otherwise had no real-time information, particularly during January 2005. The ICAO IAVW Operations Group is continuing to explore methods of increasing the frequency and reliability of pilot reports.

The encounter with SO_2 above Dili was, apart from the damage to the helicopter windscreen above Manam, the only reported aviation encounter with the eruption clouds. It was not initially reported; it only came to light after the lead author had completed a local radio interview in Darwin about the passage of the volcanic clouds near Australia (the captain of the flight happened to be listening). There is currently no ICAO requirement to report encounters with SO_2; however,

beginning November 2007 pilots will be asked to report the smell of sulfur for possible evaluation as volcanic cloud. SO_2 has a sharp odor and will sometimes be the only element reported even when ash is actually present.

When reporting of SO_2 encounters becomes an ICAO standard, we will have an opportunity to analyze more cases of encounters, and develop and deliver better guidelines to airlines for when expensive boroscope analysis should be performed to check for ash damage. Currently, most manufacturer-recommended service procedures have mandatory boroscope analyses of engines only if volcanic ash is encountered, but not if SO_2 alone has been detected. One encounter with a diffuse SO_2 cloud has been documented: the 2000 Hekla incident (Grindle and Burcham 2003) suggested engine damage where both ash and SO_2 concentrations were just below sensible levels. Conversely, we do know of at least one incident (Miyakejima, Japan, in 2000) where severe damage occurred to aircraft that flew through dense ash, but no damage was caused to aircraft that flew through the periphery of the same eruption and observed ash (Tupper et al. 2004). A possible explanation for the apparent contradiction between the Hekla and Miyakejima incidents is that the DC-8 involved in the Hekla incident spent seven minutes within the cloud (Grindle and Burcham 2003), whereas the unaffected 747 at Miyakejima exited the cloud immediately and so escaped damage.

7) WARNING CESSATION

Simpson et al. (2002) noted the difficulty of ceasing warnings abruptly when volcanic clouds become impossible to track. In 2003, the Darwin VAAC formalized an internal policy on advisory cessations:

> if ash has been successfully tracked for a number of hours, it may be possible to continue extrapolating the likely area that any ash would be contained within once it ceases to be detectable. This approach is potentially useful overnight when visible imagery is not available, or to provide a conservative ending to forecasts for situations where a significant ash cloud has been tracked for some time. One suggested approach is to shuffle the ash boundaries specified in the previous advisory forward in time so that the previous 6-hour forecast position becomes the current analysis position. If no new positions are introduced in the 18-hour forecast position, the ash boundary forecasts will naturally run their course within a few issues, at which time the advisories can be finalised (if appropriate).

This policy was generally applied to the Manam clouds, with good although imperfect success. In particular, extrapolation of the 23 November 2004 eruption cloud was not completely successful (Fig. 5a), and advisories for the 27 January 2005 cloud did not extend to Timor-Leste where the aircraft encounter took place. However, the policy provided a staged, consistent approach; appropriately extended the period for which the advisories were effective; and is a great improvement on the alternative of abrupt cessation. It is planned to continue the policy in the future.

b. Volcanic Cb avoidance

If the tentative conclusion of volcanic enhancement of the nocturnal cycle of convection is correct, and considering the much clearer diurnal enhancement at Pinatubo, an obvious avoidance strategy in convectively active situations is available to avoid encountering ash in dissipating thunderstorms. When tied to volcanic color codes for aviation and knowledge of the forecast upper winds, the strategy would be something like "Do not overfly or fly downwind of volcanoes in color code *orange* within 3 h of the normal peak in the convective cycle, and do not overfly or fly downwind of volcanoes in color code *red* at any stage." The strategy could be implemented in promptly updated or, if the volcano is already emitting ash, in SIGMETs that vary in height according to the time of day.

5. Conclusions

Six high-altitude volcanic clouds, and many more lower-level clouds, were observed from the Manam eruptions of October 2004–January 2005. One of these, on 27 January 2005, penetrated well into the stratosphere. Substantial differences in reported heights from pilots, ground observers, and satellite were found, according to the vantage point of the observers. All postanalyzed satellite heights and CO_2 slicing height comparisons were within 50 hPa, and nearly all were within 25 hPa. The eruptions were all water/ice laden and difficult to track above the freezing level using the reverse-absorption technique, except when the ice loading and small particle size of the clouds resulted in a highly positive reverse-absorption signal. Daytime reflectivity-based techniques were effective in real time and postanalysis, and SO_2 tracking of the clouds in postanalysis was very useful for validation of the warnings and advisories given. Real-time monitoring, including "hot spot" monitoring, was severely affected by cloud during January 2005. Real-time detection of volcanic lightning was attempted for these eruptions and was successful in the negative sense; the eruption clouds appeared as lightning-free zones amid areas of

active thunderstorms. A "staged" strategy of warning cessation was used to avoid abrupt warning cessation where ash could reasonably be assumed but not seen; the strategy generally worked well, but difficulties existed where the cloud could not be easily tracked and numerical guidance was poor. One aircraft encounter, an example of SO_2 olfactory fatigue, occurred over Dili, Timor-Leste, which was outside the area where analysts could confidently predict volcanic cloud. The volcanic activity appeared to cause an enhancement of the nocturnal cycle of deep convection over Manam.

To help face the challenges of the IAVW, we suggest the following:

- a continued emphasis on improving ground-based eruption prediction;
- continual experiments with aviation-funded communications, including a careful implementation of the ICAO initiative to fund volcanic observatory communications;
- implementation of real-time SO_2 detection;
- the development of guidelines for airlines for boroscope inspection (or otherwise) of aircraft engines when SO_2 has been reported but ash has not;
- continuing work on coordination procedures during high-level eruptions;
- continuing encouragement of real-time pilot reporting; and
- the implementation of avoidance strategies for dissipating volcanic-Cb, based on the possibility of volcanic ash being in the cloud, and further research into interactions between active volcanoes and convection.

Acknowledgments. We thank the staff of RVO, the PNG National Weather Service, the Darwin VAAC, Qantas, Air Niugini, Japan Airlines, Jim Mather, Peter Lawrie, Paul Hettrick, David Howard, Wally Johnson, and David Bland. The GOES and MODIS satellite data were from NOAA and NASA, respectively, and the lidar data were from the U.S. Department of Energy's Atmospheric Radiation Measurement Program. We also thank Ken Dean and two anonymous reviewers.

REFERENCES

Blong, R. J., and C. O. McKee, 1995: The Rabaul eruption, 1994—Destruction of a town. Macquarie University Natural Hazards Research Centre, New Ryde, NSW, Australia, 52 pp.

Cantor, R., 1998: Complete avoidance of volcanic ash is only procedure that guarantees flight safety. *Int. Civil Aviation Org. Mag.,* **53,** 18–19, 26.

Carn, S. A., A. J. Krueger, G. J. S. Bluth, S. J. Schaefer, N. A. Krotkov, I. M. Watson, and S. Datta, 2003: Volcanic eruption detection by the Total Ozone Mapping Spectrometer (TOMS) instruments: A 22-year record of sulfur dioxide and ash emissions. *Volcanic Degassing,* C. Oppenheimer, D. M. Pyle, and J. Barclay, Eds., Geological Society of London, 177–202.

Coakley, J. A., and F. P. Bretherton, 1982: Cloud cover from high-resolution scanner data: Detecting and allowing for partially filled fields of view. *J. Geophys. Res.,* **87,** 4917–4932.

Constantine, E. K., G. J. S. Bluth, and W. I. Rose, 2000: TOMS and AVHRR observations of drifting volcanic clouds from the August 1991 eruptions of Cerro Hudson. *Remote Sensing of Active Volcanism, Geophys. Monogr.,* Vol. 116, Amer. Geophys. Union, 45–64.

Davidson, N. E., and K. Puri, 1992: Tropical prediction using dynamical nudging, satellite-defined convective heat sources, and cyclone bogus. *Mon. Wea. Rev.,* **120,** 2501–2522.

Draxler, R. R., and G. D. Hess, 1998: An overview of the Hysplit_4 modeling system for trajectories, dispersion, and deposition. *Aust. Meteor. Mag.,* **47,** 295–308.

Fromm, M., A. Tupper, D. Rosenfeld, R. Servranckx, and R. McRae, 2006: Violent pyro-convective storm devastates Australia's capital and pollutes the stratosphere. *Geophys. Res. Lett.,* **33,** L05815, doi:05810.01029/02005GL025161.

Grindle, T. J., and F. W. Burcham, 2003: Engine damage to a NASA DC-8-72 airplane from a high-altitude encounter with a diffuse volcanic ash cloud. NASA Tech. Memo. NASA/TM-2003-212030, 22 pp.

Hoblitt, R. P., and T. L. Murray, 1990: Lightning detection and location as a remote eruptions monitor at Redoubt Volcano, Alaska. *Eos, Trans. Amer. Geophys. Union,* **71,** 146.

Holasek, R. E., S. Self, and A. W. Woods, 1996: Satellite observations and interpretation of the 1991 Mount Pinatubo eruption plumes. *J. Geophys. Res.,* **101,** 27 635–27 665.

Innes, D., 2004: Air Niugini and the volcanic ash threat. *Proc. Second Int. Conf. on Volcanic Ash and Aviation Safety,* Alexandria, VA, Office of the Federal Coordinator for Meteorological Services and Supporting Research, 1:15–16.

International Civil Aviation Organization, 2001: Manual on Volcanic Ash, Radioactive Material and Toxic Chemical Clouds, ICAO Doc. 9691-AN/954, appendix I.

——, 2006: Handbook on the International Airways Volcano Watch (IAVW). 2d ed. 46 pp. [Available online at http://www.icao.int/icao/en/anb/met/index.html.]

Johnson, R. W., and T. J. Casadevall, 1994: Aviation safety and volcanic ash clouds in the Indonesia-Australia region. *Proc. First Int. Symp. on Volcanic Ash and Aviation Safety,* Seattle, WA, Office of the Federal Coordinator for Meteorological Services and Supporting Research, 191–197.

Kinoshita, K., C. Kanagaki, N. Iino, M. Koyamada, A. Terada, and A. Tupper, 2002: Volcanic plumes at Miyakejima observed from satellites and from the ground. *Proc. SPIE,* **4891,** 227–236.

Krueger, A. J., L. S. Walter, P. K. Bhartia, C. C. Schnetzler, N. A. Krotkov, I. Sprod, and G. J. S. Bluth, 1995: Volcanic sulphur dioxide measurements from the Total Ozone Mapping Spectrometer (TOMS) instruments. *J. Geophys. Res.,* **100,** 14 057–14 076.

Mapes, B. E., T. T. Warner, and M. Xu, 2003: Diurnal patterns of rainfall in northwestern South America. Part III: Diurnal gravity waves and nocturnal convection offshore. *Mon. Wea. Rev.,* **131,** 830–844.

Mayberry, G. C., W. I. Rose, and G. J. S. Bluth, 2003: Dynamics of

the volcanic and meteorological clouds produced by the December 26, 1997 eruption of Soufrière Hills volcano, Montserrat, W.I. *The Eruption of Soufrière Hills Volcano, Montserrat, 1995–99,* T. Druitt and P. Kokelaar, Eds., Geological Society of London, 539–555.

Menzel, W. P., W. L. Smith, and T. R. Stewart, 1983: Improved cloud motion wind vector and altitude assignment using VAS. *J. Climate Appl. Meteor.,* **22,** 377–384.

Oswalt, J. S., W. Nichols, and J. F. O'Hara, 1996: Meteorological observations of the 1991 Mount Pinatubo eruption. *Fire and Mud: Eruptions and Lahars of Mount Pinatubo, Philippines,* C. G. Newhall and R. S. Punongbayan, Eds., Philippines Institute of Volcanology and Seismology and University of Washington Press, 625–636.

Palfreyman, W. D., and R. J. S. Cooke, 1976: Eruptive history of Manam volcano, Papua New Guinea. *Volcanism in Australasia,* R. W. Johnson, Ed., Elsevier Scientific, 117–128.

Platnick, S., M. D. King, S. A. Ackerman, W. P. Menzel, B. A. Baum, J. C. Riédi, and R. A. Frey, 2003: The MODIS cloud products: Algorithms and examples from Terra. *IEEE Trans. Geosci. Remote Sens.,* **41,** 459–473.

Potts, R. J., 1993: Satellite observations of Mt Pinatubo ash clouds. *Aust. Meteor. Mag.,* **42,** 59–68.

Prabhakara, C., and J. M. Yoo, 1990: Remote sensing over oceans of optically thin cirrus and its significance. *Proc. SPIE,* **1299,** 154–173.

Prata, A. J., 1989a: Infrared radiative transfer calculations for volcanic ash clouds. *Geophys. Res. Lett.,* **16,** 1293–1296.

——, 1989b: Observations of volcanic ash clouds in the 10–12 μm window using AVHRR/2 data. *Int. J. Remote Sens.,* **10,** 751–761.

——, and C. Bernardo, 2007: Retrieval of volcanic SO_2 total column from AIRS data. *J. Geophys. Res.,* in press.

——, W. I. Rose, S. Self, and D. M. O'Brien, 2003: Global, long-term sulphur dioxide measurements from TOVS data: A new tool for studying explosive volcanism and climate. *Volcanism and the Earth's Atmosphere, Geophys. Monogr.,* Vol. 139, Amer. Geophys. Union, 75–92.

Rose, W. I., and Coauthors, 1995: Ice in the 1994 Rabaul eruption cloud: Implications for volcano hazard and atmospheric effects. *Nature,* **375,** 477–479.

Rosenfeld, D., and I. M. Lensky, 1998: Spaceborne sensed insights into precipitation formation processes in continental and maritime clouds. *Bull. Amer. Meteor. Soc.,* **79,** 2457–2476.

Rudich, Y., A. Sagi, and D. Rosenfeld, 2003: Influence of the Kuwait oil fires plume (1991) on the microphysical development of clouds. *J. Geophys. Res.,* **108,** 4478, doi:4410.1029/2003JD003472.

Sawada, Y., 1987: Study on analysis of volcanic eruptions based on eruption cloud image data obtained by the Geostationary Meteorological Satellite (GMS). Meteorological Research Institute Tech. Rep. 22, Tsukuba, Japan, 335 pp.

Schneider, D. J., and W. I. Rose, 1994: Observations of the 1989–90 Redoubt volcano eruption clouds using AVHRR satellite imagery. *Volcanic Ash and Aviation Safety,* T. J. Casadevall, Ed., U.S. Geological Survey, 405–418.

Seemann, S. W., J. Li, L. E. Gumley, and W. P. Menzel, 2003: Operational retrieval of atmospheric temperature, moisture, and ozone from MODIS infrared radiances. *J. Appl. Meteor.,* **42,** 1072–1091.

Simpson, J. J., G. L. Hufford, D. Pieri, R. Servranckx, J. S. Berg, and C. Bauer, 2002: The February 2001 eruption of Mount Cleveland, Alaska: Case study of an aviation hazard. *Wea. Forecasting,* **17,** 691–704.

Textor, C., H. Graf, M. Herzog, and J. M. Oberhuber, 2003: Injection of gases into the stratosphere by explosive volcanic eruptions. *J. Geophys. Res.,* **108,** 4606, doi:4610.1029/2002JD002987.

Torres, O., P. K. Bhartia, J. R. Herman, Z. Ahmad, and J. Gleason, 1998: Derivation of aerosol properties from satellite measurements of backscattered ultraviolet radiation: Theoretical basis. *J. Geophys. Res.,* **103,** 17 099–17 110.

Tupper, A., and K. Kinoshita, 2003: Satellite, air and ground observations of volcanic clouds over islands of the southwest Pacific. *South Pac. Study,* **23,** 21–46.

——, S. Carn, J. Davey, Y. Kamada, R. Potts, F. Prata, and M. Tokuno, 2004: An evaluation of volcanic cloud detection techniques during recent significant eruptions in the western 'Ring of Fire.' *Remote Sens. Environ.,* **91,** 27–46.

——, J. S. Oswalt, and D. Rosenfeld, 2005: Satellite and radar analysis of the volcanic-cumulonimbi at Mount Pinatubo, Philippines, 1991. *J. Geophys. Res.,* **110,** D09204, doi:10.1029/2004JD005499.

University of Wisconsin—Madison, cited 2005: McIDAS (Man computer Interactive Data Access System). [Available online at http://www.ssec.wisc.edu/mcidas/.]

Watkin, H. A., T. R. Scott, I. Macadam, L. C. Radice, and D. J. Hoad, 2003: Reducing the false alarm rate of a Met Office automatic volcanic eruption detection system. Forecasting Research Tech. Rep. 414, Met Office, Exeter, Devon, United Kingdom, 19 pp.

Wielicki, B. A., and J. A. J. Coakley, 1981: Cloud retrieval using infrared sounder data: Error analysis. *J. Appl. Meteor.,* **20,** 157–169.

Wright, R., L. P. Flynn, H. Garbeil, A. J. L. Harris, and E. Pilger, 2002: Automated volcanic eruption detection using MODIS. *Remote Sens. Environ.,* **82,** 135–155.

Wunderman, R., 2004: Sulfurous odors: A signal of entry into an ash plume: perhaps less reliable for escape. *Proc. Second Int. Conf. on Volcanic Ash and Aviation Safety,* Alexandria, VA, Office of the Federal Coordinator for Meteorological Services and Supporting Research, P1.2.

Wylie, D. P., W. P. Menzel, H. M. Woolf, and K. I. Strabala, 1994: Four years of global cirrus cloud statistics using HIRS. *J. Climate,* **7,** 1972–1986.